

Proceedings of the ASME 2023 18th International Manufacturing Science and Engineering Conference MSEC2023

June 12-16, 2023, New Brunswick, NJ, USA

MSEC2023-106259

SPATIAL-TERMINAL ITERATIVE LEARNING CONTROL FOR REGISTRATION ERROR ELIMINATION IN HIGH-PRECISION ROLL-TO-ROLL PRINTING SYSTEMS

Zifeng Wang, Xiaoning Jin*

Northeastern University, Boston, MA

ABSTRACT

Roll-to-roll (R2R) printing techniques are promising for high-volume continuous production of substrate-based electronic products, as opposed to the sheet-to-sheet approach suited for low-volume work. However, one of the major challenges in R2R flexible electronics printing is achieving tight alignment tolerances, as specified by the device resolution (usually at micrometer level), for multi-layer printed electronics. The alignment of the printed patterns in different layers, known as registration, is critical to product quality. Registration errors are essentially accumulated positional or dimensional deviations caused by undesired variations in web tensions and web speeds. Conventional registration control methods rely on model-based feedback controllers, such as PID control, to regulate the web tension and the web speed. However, those methods can not guarantee that the registration error always converges to zero due to lagging problems. In this paper, we propose a Spatial-Terminal Iterative Learning Control (STILC) method combined with PID control to enable the registration error to converge to zero iteratively, which achieves unprecedented control in the creation, integration and manipulation of multi-layer microstructures in R2R processes. We simulate the registration error generation and accumulation caused by axis mismatch between roller and motor that commonly exists in R2R systems. We show that the STILC-PID hybrid control method can eliminate the registration error completely after a reasonable number of iterations. We also compare the performances of STILC with a constant-value basis and a cosine-form basis. The results show that the control model with a cosine-form basis provides a faster convergence speed for R2R registration error elimination.

Keywords: Roll-to-roll printing systems, Registration error, Spatial iterative learning control, Terminal iterative learning control

1. INTRODUCTION

Roll-to-roll (R2R) printing systems are promising for manufacturing substrate-based products in a high-throughput and continuous manner, as opposed to sheet-to-sheet approach suited for low-volume work. In R2R printing systems, registration error is a crucial factor that influences the quality of final products which need to meet a tight tolerance requirement. The registration error is defined as the misalignment of the printed patterns on different layers. To guarantee the functionality of the products manufactured by an R2R printing system, it is important to eliminate layer-wise misalignment of the printed patterns through effective registration control. However, the registration error can only be measured after the downstream pattern is printed [1–3], making it infeasible to monitor the intermediate state of the registration error in real-time. This limitation of real-time monitoring capability results in difficulties in R2R registration control.

Fluctuations in both web tensions and web speeds in an R2R printing system are the root causes of registration errors by deviating the printed patterns from the desired positions on the moving web [4–6]. Because web tensions and speeds are continuously accessible in real-time, some feedback control methods are proposed to reduce the registration error by regulating web tensions and speeds in R2R printing systems [4, 7, 8]. However, these feedback control methods are considered indirect control strategies. They are unable to completely eliminate the registration error which is resulted from the accumulative effect of tension and speed fluctuations in each operation cycle (rotational cycle of printing roller). Even if feedback controllers can make the tension and speed converge to their reference values at the end of each operation cycle, the registration error for each operation cycle is not zero as an accumulative quantity measured at the end of the operation cycle. The value of the output variable at the end of each operation cycle is defined as the terminal output of this operation cycle. Therefore, registration error is a class of terminal outputs for R2R processes. Due to the fact that the R2R printing operation cycle is repeated for massive production, disturbances in tensions and speeds may also occur repetitively. As a result, even if those feedback control methods can reduce

^{*}Corresponding author: xi.jin@northeastern.edu
Documentation for asmeconf.cls: Version 1.32, March 19, 2023.

the registration error to a nonzero level, they cannot completely eliminate the registration error. Those feedback control methods may not be satisfying in some scenarios requiring high-precision printing registration control, such as multi-layer printed electronic devices.

Iterative learning control (ILC) is a class of control methods designed for repetitive manufacturing processes [9]. Compared to conventional feedback control methods such as proportional-integral-derivative (PID) control, ILC displays a superior learning ability by iteratively adjusting the control input profiles for the repetitive operation cycles based on historical data from previous cycles. The operation cycle is defined as iteration in ILC. In some previous studies[10, 11], ILC methods are designed to mitigate transient behaviors in R2R processes by regulating the web tensions iteratively. However, they require that the desired tension profile for each cycle is known as prior knowledge. In practice, it is more typical for applications to tolerate slight deviations in tensions during the cycle while closely monitoring the register error, which is the terminal output (i.e., the output at the end of the cycle). When only the terminal output of each iteration is measurable, Terminal Iterative Learning Control (TILC) methods are designed in [12-15] to update the control input profile iteratively from only the terminal output instead of the entire output profile. In TILC, the input profile for the current iteration is decided by the terminal output of the last iteration and a predefined basis function. The basis function is desired to provide an exactly opposite input signal to compensate for the disturbance. When the basis function provides a profile severely deviating from the desired one, the TILC method will suffer from instabilities and slower convergences, or even failures. Therefore, it is critical to construct a proper basis function for TILC to guarantee good control performance. [15] shows a constant-value basis function to simplify the controller design, but it is not able to make use of any information about the controlled system. [16] designs a basis function vector with three basis function components for an RTPCVD system based on a well-known state-space model of the system. To further improve the control performance, some papers construct basis functions that can be updated by data-driven approaches, such as iterative dynamical linearization [12–14] and neural-network-based methods [15]. However, iterative updating mechanisms are computationally expensive and not applicable to most real-time control problems. In this paper, in order to achieve both good control performance and less computational burden, we look into the known knowledge about the controlled system to design a proper basis function.

The disturbances in systems equipped with rotary components such as spindles in lathing, milling, and grinding processes, as well as rollers in R2R systems, are often dependent on angular displacements of rotating devices because of circular behavior of such systems [17]. The idea of Spatial Iterative Learning Control (SILC) has been proposed and demonstrated in many applications such as 3D printing processes [18], wind turbines [19], and robotic arms [20]. For SILC, the iterative updating law built upon basic ILC scheme is constructed in the spatial domain instead of the temporal domain, which demonstrated the expanded capability of iterative learning by an alternative definition of "iteration". In this paper, we design a cosine-form basis function for

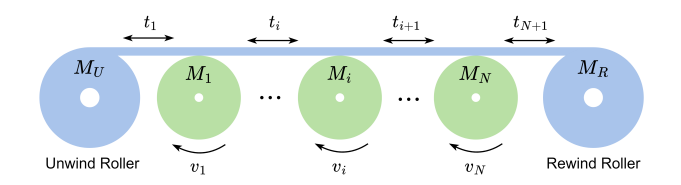


FIGURE 1: A GENERAL R2R PRINTING SYSTEM WITH UNWIND, REWIND, AND INTERMEDIATE ROLLERS

the spatial information representation (phase angle of the printing roller) under the SILC framework. With the space-dependent basis function, we propose a Spatial-Terminal Iterative Learning Control (STILC) method combined with a decentralized PID controller [7] to achieve effective registration control for R2R printing. The main advantages of the proposed STILC method are listed as the following:

- (1) The proposed STILC method can enable the registration error to converge to zero iteratively.
- (2) The proposed STILC method only requires the terminal output of each iteration (the registration error at the end of each rotational cycle) to update the input profile. Thus it can work in R2R registration control problems without continuous-time monitoring of the registration error.
- (3) The proposed STILC method uses a cosine-form basis function in terms of roller phase angle to compensate for the angle-dependent repetitive disturbances in rotary machine systems.

The remainder of this paper is organized as follows. Section 2 establishes the physics-based model of the R2R registration error using the perturbation-based approximation method. Section 3 presents the STILC-PID hyrbrid controller design in details and demonstrate its performance in terms of registration error control effectiveness and speed of convergence by experimenting with different system parameters and various scenarios of angle-dependent repetitive disturbance in simulations. Section 4 concludes the paper.

2. PHYSICAL MODEL OF THE REGISTRATION ERROR IN R2R SYSTEMS

2.1 Dynamics of the web handling system

A typical R2R printing system includes a web handling system transporting the flexible web (substrate) through a series of rollers. In this paper, we study the R2R printing system with gravure printing rollers. Figure 1 shows an R2R system with one unwinding roller (M_U) , one rewinding roller (M_R) , and N intermediate rollers $(M_1 - M_N)$.

For further discussion, we make the following two assumptions.

A1: There is no slippage between the roller and the web [6, 7]. In other words, the tangential roller speeds $(v_i, i = 1, 2, ..., N)$ are equal to the speeds of the following web span. The web span is defined as the web section between two successive rollers.

A2: The web tension t_i , $i \in \{1, 2, ..., N+1\}$ and web speed v_i , $i \in \{1, 2, ..., N\}$ are constant through a span.

Based on [7], we can analyze the dynamics of each intermediate roller as shown in Fig. 2.

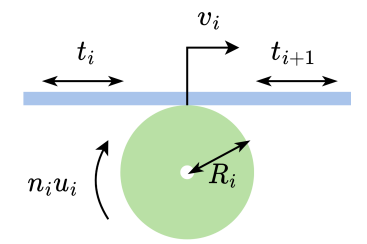


FIGURE 2: DYNAMICS OF ONE INTERMEDIATE ROLLER

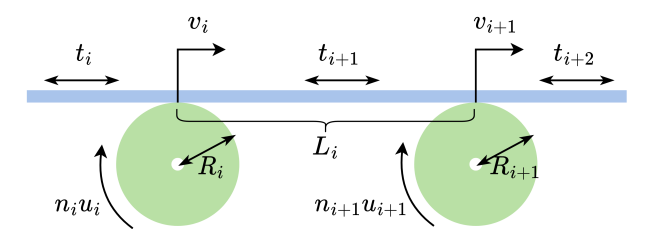


FIGURE 3: DYNAMICS OF TWO SUCCESSIVE PRINTING ROLLERS

The dynamics are described by the following differential equation:

$$\frac{J_i}{R_i}\dot{v}_i = (t_{i+1} - t_i)R_i + n_i u_i - \frac{f_i}{R_i}v_i \tag{1}$$

where J_i , R_i , n_i , and f_i are the inertia, radius, gearing ratio, and friction coefficient of roller i, respectively. u_i is the torque input provided by the motor of roller i. $i \in \{1, 2, ..., N\}$ is the index of the roller.

Some of the intermediate rollers can be assigned to work as printing rollers. In this paper, the registration error is defined as the distance between the two printed patterns printed by two successive printing rollers. Thus, we extend the analysis in Fig. 2 to the case including two successive printing rollers, as shown in Fig. 3.

For a two-roller system, we can derive the dynamic equations for v_i and v_{i+1} , and the dynamic equations for the tension through the web span between these two rollers [7]. The dynamic equations for the tension are

$$L_i \dot{t}_i = AE(v_i - v_{i-1}) + t_{i-1} v_{i-1} - t_i v_i \tag{2}$$

where L_i is the span length, A is the cross-sectional area of the substrate, E is the elastic modulus of the substrate.

To convert the dynamic equations to perturbation form [7], we define some perturbation variables:

$$v_i(\tau) = v_i^r + V_i(\tau)$$

$$t_i(\tau) = t_i^r + T_i(\tau)$$

$$u_i(\tau) = u_i^r + U_i(\tau)$$
(3)

where τ denotes time. v_i^r and t_i^r are speed and tension references. V_i and T_i are the variations (perturbation variables) in speed and tension. u_i^r is the equilibrium control input to maintain the speed and tension at the given reference levels. u_i^r can be calculated as follows:

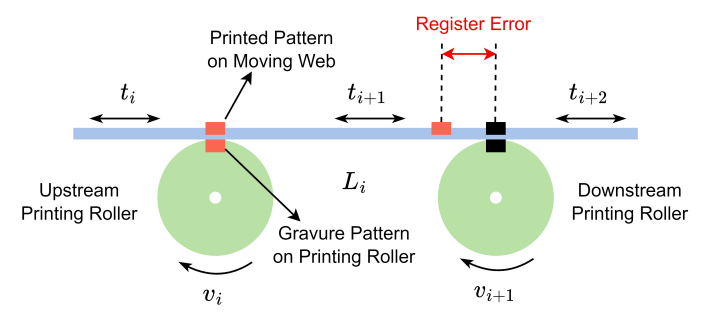


FIGURE 4: REGISTRATION ERROR IN A TWO-ROLLER PRINTING UNIT

$$u_i^r = \frac{f_i}{n_i R_i} v_i^r - \frac{R_i}{n_i} (t_{i+1}^r - t_i^r)$$
 (4)

Then we can derive the dynamic equations for the two-roller case in perturbation form:

$$\begin{cases} \frac{J_{j}}{R_{j}}\dot{V}_{j} = (T_{j+1} - T_{j})R_{j} + n_{j}U_{j} - \frac{f_{j}}{R_{j}}V_{j} & j = i, i+1, \\ L_{k}\dot{T}_{k} = AE(V_{k} - V_{k-1}) \\ + (t_{k-1}^{r}V_{k-1} + v_{k-1}^{r}T_{k-1}) - (t_{k}^{r}V_{k} + v_{k}^{r}T_{k}) \\ + (t_{k-1}^{r}v_{k-1}^{r} - t_{k}^{r}v_{k}^{r}) & k = i, i+1, i+2 \end{cases}$$

$$(5)$$

Note that Eq. (5) includes state variables v_{i-1} and t_{i-1} that are not shown in Fig. 3 but exist in Fig. 1. To simplify the control problem, we assume that in an R2R system shown in Fig. 1, tensions and speeds of the rollers except for the printing rollers M_i and M_{i+1} are well-controlled and always equal to the reference values. Therefore, the whole system can be described by Eq. (5) with the five state variables $(V_i, V_{i+1}, T_i, T_{i+1}, T_{i+2})$. Thus, when we establish the model for general R2R systems as shown in Fig. 1, we can ignore the other parts except the two-roller section shown in Fig. 3.

2.2 Mathematical model of the registration error

We now present the dynamic model of the R2R registration error. Figure 4 shows the schematic of two adjacent gravure printing rollers. The red squares represent the patterns printed by the upstream roller. The black square represents the pattern printed by the downstream roller. The registration error is defined as the distance between the two patterns printed by the upstream roller and the downstream roller respectively. Without loss of generality, we make the following assumption on the span length.

A3: The span length between the two printing rollers is equal to the circumference of the upstream roller. $(L_i = 2\pi R_i)$

By A3, we know that when the substrate is running with steady tension and speed, the pattern printed by the downstream roller (black square) should coincide with the pattern printed previously by the upstream roller (red square). When there are fluctuations in tension and speed caused by internal or external disturbances, the misalignment between the two printed patterns will occur.

From [6], the relationship between the registration error and the variations of web speeds and web tensions can be linearized by a perturbation method and described as the following differential equation:

$$\dot{r_i}(\tau) = \frac{1}{AE} \left[v_i^r T_i(\tau - \tau_i^r) - v_{i+1}^r T_{i+1}(\tau) \right]$$
 (6)

where r_i is the registration error generated by printing roller i and printing roller i+1, τ_i^r is the reference time interval for the upstream printed pattern to be transported to the downstream roller. τ_i^r can be the actual time interval when v_i is equal to v_i^r constantly. If v_i is varying, the time interval may also change. To simplify the problem, we make the following assumption. A4: The variations of tension and speed are relatively small.

With A4, we know that the actual time interval should be very close to τ_i^r . Thus, we can treat it as a constant value in Eq. (6).

Under A1-A4, Equations (5) and (6) describe the state-space model of the R2R registration error problem as a linear system. The input variables are the motor torque variations of the two printing rollers. The output variable is the registration error. The state variables are the variations of the speeds (V_i, V_{i+1}) and tensions (T_i, T_{i+1}) .

Remark 1. The process of generating the registration error is repetitive. Each time the pattern is printed, the last operation cycle is terminated and a new operation cycle starts. This is why ILC is considered a suitable approach for such repetitive processes.

Remark 2. It should be noted that even though r_i is the variable representing registration error, the actual registration error is only generated every time the downstream pattern is printed. Therefore, the registration error is only measured every time the printing roller completes a cycle. During the cycle, there is no continuous measurement of the registration error. This is the reason for us to design the terminal ILC method for R2R registration control.

3. CONTROLLER DESIGN AND SIMULATION RESULTS

3.1 Design of the STILC-PID hybrid controller

In [7], a decentralized controller is designed for regulating the speeds and tensions in the R2R system. Figure 5 shows the schematic of the decentralized control scheme for a two-roller system. The control input signal for each roller motor is the summation of two components: (a) the open-loop component given by Eq. (4), and (b) the closed-loop component generated by a PID controller.

The control law of the decentralized controller is given as the following:

$$u_{j}(\tau) = u_{j}^{OL} + u_{j}^{PID}(\tau)$$

$$u_{j}^{OL} = u_{j}^{r}$$

$$u_{j}^{PID}(\tau) = K_{j}^{P} \begin{bmatrix} T_{j}(\tau) & V_{j}(\tau) \end{bmatrix}^{T}$$

$$+ K_{j}^{I} \begin{bmatrix} \int_{0}^{\tau} T_{j}(\tau) d\tau & \int_{0}^{\tau} V_{j}(\tau) d\tau \end{bmatrix}^{T}$$

$$+ K_{j}^{D} \begin{bmatrix} \dot{T}_{j}(\tau) & \dot{V}_{j}(\tau) \end{bmatrix}^{T}$$

$$(7)$$

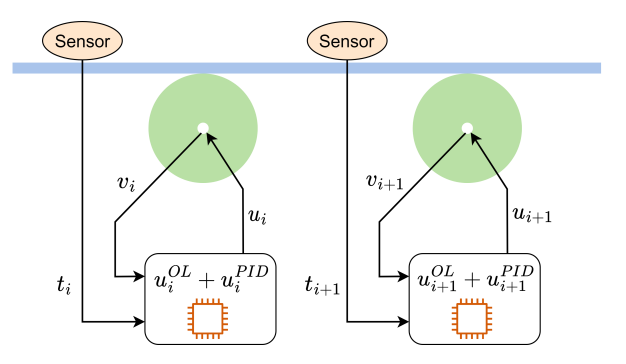


FIGURE 5: DECENTRALIZED PID CONTROL FOR TENSION AND SPEED REGULATION

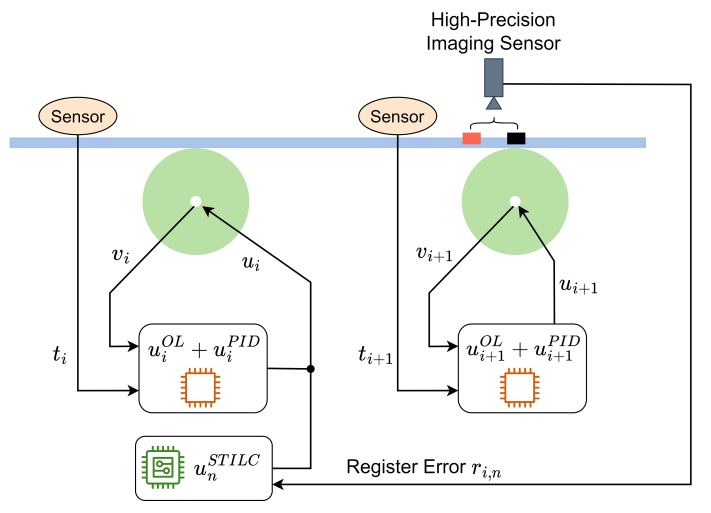


FIGURE 6: STILC-PID HYBRID CONTROL FOR REGISTRATION ERROR

where j = i, i + 1, u_j^{OL} is the open-loop input component, u_j^{PID} is the closed-loop input component provided by the PID controller, and K_i is the feedback gain vector.

In this paper, a disturbance is introduced to the upstream roller to test out the control algorithm. The disturbance is dependent on the phase angle of the gravure pattern on the upstream roller. This motivates us to design a TILC based on spatial information (phase angle) instead of a traditional temporal TILC to compensate for the disturbance. The details of this phase-dependent disturbance will be discussed in Section 3.2. Figure 6 shows the schematic of the two-roller R2R printing system with the hybrid controller including a decentralized PID controller and a STILC controller for the upstream roller.

The control law of the hybrid controller is given as follows:

$$u_j(\tau) = u_j^{OL} + u_j^{PID}(\tau) + u_n^{STILC}(\theta_i(\tau))$$
 (8)

where u_n^{STILC} is the STILC input component generated by the STILC controller, n is the iteration index in the STILC controller, θ_i is the phase angle of the gravure pattern on the upstream roller. The iterative updating law for STILC is designed based on the P-type ILC updating law:

$$u_{n+1}^{STILC}(\theta_i) = u_n^{STILC}(\theta_i) + PG(\theta_i)r_{i,n} \tag{9}$$

TABLE 1: SIMULATION PARAMETERS

Parameter	Notation	Value
Cross-sectional Area	A	$1.29 \times 10^{-5} \ m^2$
Young's Modulus	E	186.158 MPa
Reference Roller Radius	R_i^r, R_{i+1}	0.381 m
Inertia of Roller	J_i, J_{i+1}	$0.146 \ kg \cdot m^2$
Friction Coefficient	f_i, f_{i+1}	0.685
Gear Ratio	n_i, n_{i+1}	1
Span Length	L_i,L_{i+1},L_{i+2}	2.4 m
Reference Speed	v_i^r, v_{i+1}^r	0.16 m/s
Reference Tension	$t_{i}^{r}, t_{i+1}^{r}, t_{i+2}^{r}$	20 N
Reference Period Time	$ au_i^r$	14.962 s

where $u_{n+1}^{STILC}(\theta_i)$ is the STILC control input component when the phase angle is θ_i for the $(n+1)^{th}$ iteration (current iteration), $u_n^{STILC}(\theta_i)$ is the STILC control input at the same phase angle for the nth iteration (last iteration), P is the learning gain, G is the basis function, $r_{i,n}$ is the registration error generated in the nth iteration (last iteration).

The phase angle θ_i is a function of time and can be calculated by the following integral:

$$\theta_i(\tau) = \int_0^\tau \frac{v_i^r + V_i}{R_i} d\tau \tag{10}$$

With Eqs. (8)(9)(10), we complete the hybrid controller design. Comparing our design to the existing decentralized controller, we add a STILC input component to the control input for the upstream printing roller. Next, we will show the effectiveness of the hybrid controller in R2R registration control with the simulation results from a numerical experiment.

3.2 Simulation results

We establish the numerical model of the R2R printing system in Simulink and set the parameters as shown in Table 1.

In R2R systems, axis mismatch phenomena commonly occur between the motor shaft and the geometric center of the roller, which causes a periodic disturbance for the repetitive rotary process [17]. In this simulation, we set an axis mismatch in the upstream printing roller. When the mismatch exists, the effect of this eccentric printing roller is equivalent to a roller with its radius varying over the phase angle. We define the angle-varying radius as the equivalent radius of the roller with respect to the phase angle. Therefore, the parameter R_i is transferred to a function of the phase angle:

$$R_i(\theta_i) = R_i^r + e \cos(\theta_i) \tag{11}$$

where R_i^r is the constant value of the original radius when there is no axis mismatch, e is the eccentricity defined as the distance between the motor shaft and the roller center. Figure 7 shows how the equivalent radius R_i varies with respect to the phase angle through an operation cycle.

This disturbance is introduced in the simulation experiments. However, in practical applications, this disturbance profile is not known as prior knowledge when we design the hybrid controller.

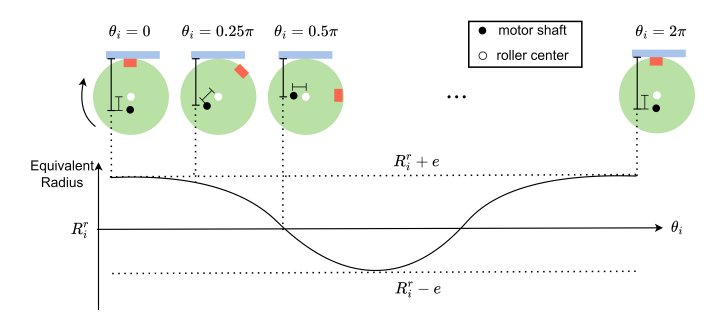


FIGURE 7: PHASE-ANGLE-VARYING EQUIVALENT RADIUS CAUSED BY AXIS MISMATCH

Thus, the open-loop component of the control input is still a constant value

$$u_i^{OL} = \frac{f_i}{n_i R_i^r} v_i^r - \frac{R_i^r}{n_i} (t_{i+1}^r - t_i^r)$$
 (12)

while the desired control input should be designed to maintain the force equilibrium as follows:

$$u_{i}^{r} = \frac{f_{i}}{n_{i}R_{i}(\theta_{i}(\tau))}v_{i}^{r} - \frac{R_{i}(\theta_{i}(\tau))}{n_{i}}(t_{i+1}^{r} - t_{i}^{r})$$
(13)

Therefore, if we only input the open-loop component to the system, the control input will deviate from the desired input profile and result in fluctuations in tension and speed, causally generating the registration error at the end of each iteration. By Eq. (3), the perturbation of the input variable U_i should be

$$U_i(\tau) = u_i(\tau) - u_i^r(\tau)$$

$$= u_i^{OL} - u_i^r(\tau)$$
(14)

Note that R_i is also included explicitly in Eq. (5) and Eq. (10). Those R_i 's should also be substituted by Eq. (11).

We realize the R2R system modeling and the disturbance introduction in Simulink. Figure 8 shows the fluctuations of the five state variables in Eq. (5) in time domain when we introduce the axis mismatch to the upstream roller. Note that T_{i+1} and T_{i+2} are overlapping. Figure 9 shows the registration error caused by the fluctuations in speed and tension. Note that $r_i(\tau)$ is a continuous function of time, but it can only be measured by the sensor when the downstream pattern hasn't been printed on the web. Therefore, the value of the actual registration error is updated each time the terminal condition is satisfied, that is when the phase angle of the gravure pattern on the downstream roller reaches 2π . During the intermediate process of each iteration, the registration error keeps constant after being updated at the beginning of the iteration. As shown in Fig. 9b, the registration error accumulates and dilates iteratively when we only apply the open-loop input component to the system.

Figure 10 shows the comparison between the registration control performances when different control methods are applied. The controller settings are given in Table 2. The simulation results show that the decentralized PID control method makes the registration error converge to a non-zero level. Compared to the decentralized PID control method, the proposed hybrid controller

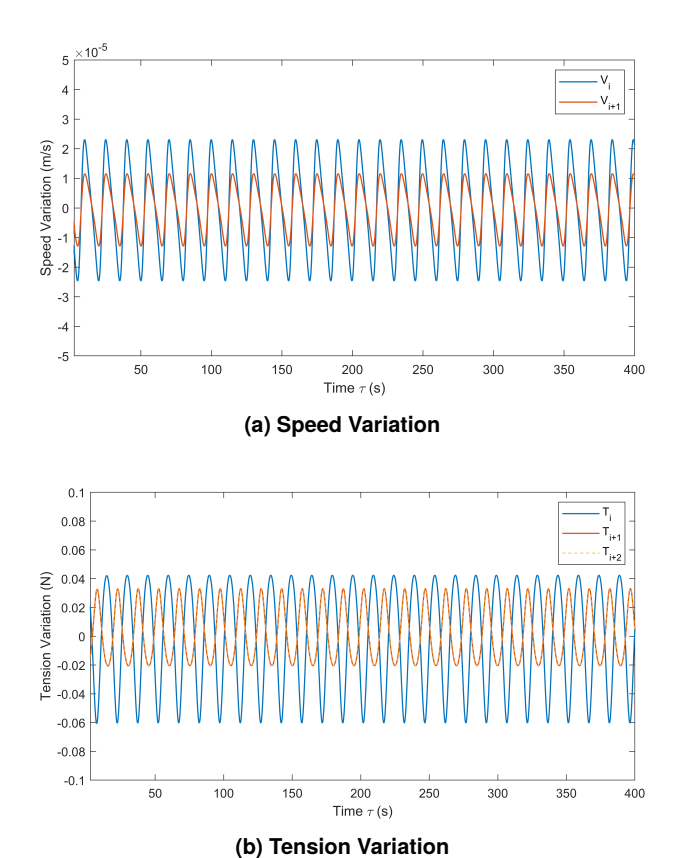
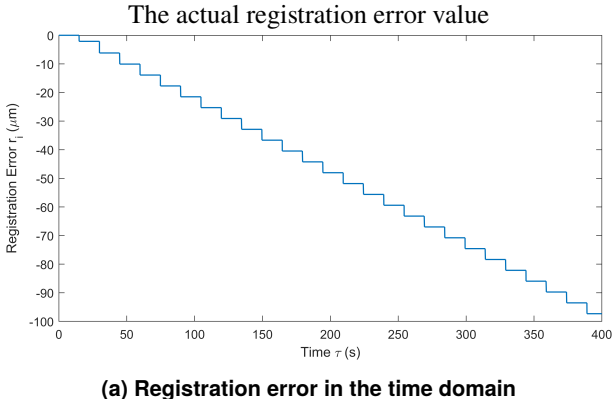
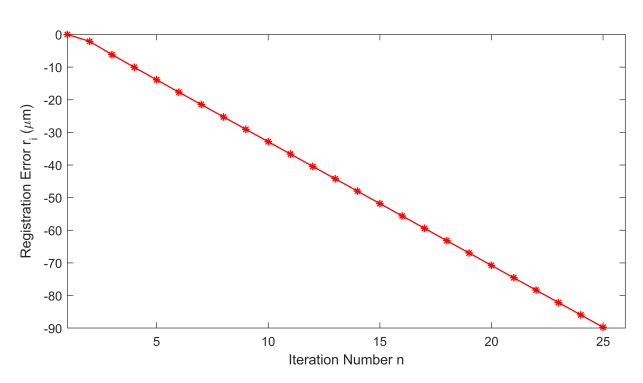


FIGURE 8: SPEED AND TENSION VARIATIONS CAUSED BY AXIS **MISMATCH**

with an extra STILC input component makes the registration error converge to zero after sufficient iterations (11 iterations in this simulation case). Therefore, the proposed hybrid controller shows its significant advantage in R2R printing registration control.

We also compare the performances of three STILC controllers with different basis functions. A common basis function for TILC updating law is a time-invariant function, which means the value of the basis function keeps constant during each iteration [15]. This is the easiest one to realize, but it cannot make use of any physical knowledge we have about the R2R printing process. To adjust to the problem in this paper, we substitute the constant-value basis function with a cosine function. It should be noted that the ideal basis function should provide a compensated signal with exactly the same form of the U_i fluctuation given in Eq. (14). But it is much more difficult for practitioners to find the mathematical function for the U_i fluctuation. By comparison, it is feasible for people to use a cosine basis function when they assume the disturbance is introduced by axis mismatch. To make the STILC more feasible in real-world scenarios, we also design a discretized basis function as shown in Fig. 11. The discretized basis function can be written in the memory of the controller as a small lookup table. Thus, it can help avoid computing the cosine function in real-time. Figure 12 shows that the discretized cosine-form basis functions can help the controller to make the registration error converge to zero iteratively. The cosine-form basis function with more discretization steps provides faster con-





(b) Registration error in iteration domain

FIGURE 9: REGISTER ERROR CAUSED BY AXIS MISMATCH WITH **ONLY OPEN-LOOP CONTROL INPUT**

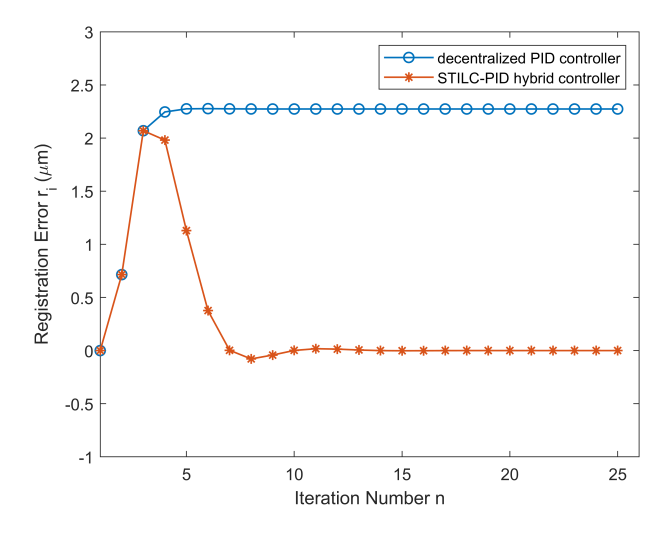


FIGURE 10: PERFORMANCE COMPARISON BETWEEN PRO-POSED STILC-PID HYBRID CONTROLLER AND TRADITIONAL **CONTROLLERS**

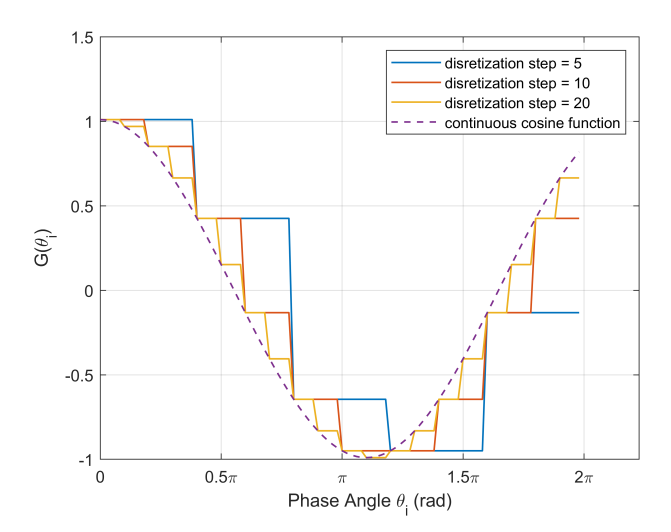


FIGURE 11: DISCRETIZED COSINE-FORM BASIS FUNCTIONS WITH DIFFERENT DISCRETIZATION STEP

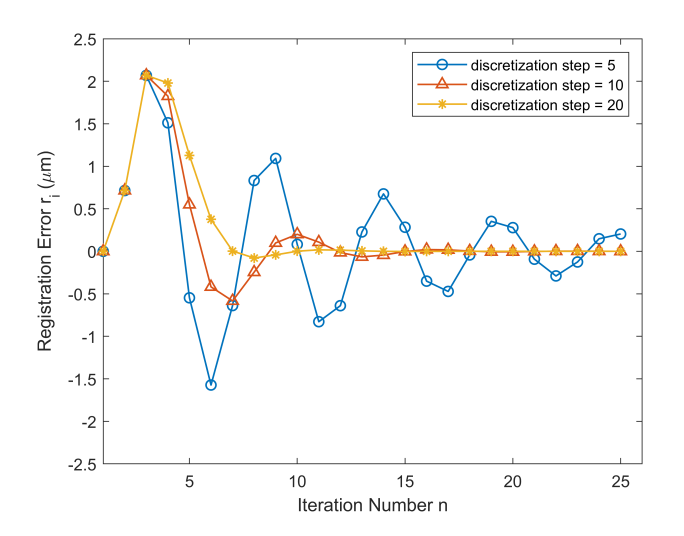


FIGURE 12: PERFORMANCE COMPARISON BETWEEN STILC-PID HYBRID CONTROLLERS WITH DIFFERENT BASIS FUNCTION

vergence speed. Therefore, we can use the discretized cosine basis function with 20 discretization steps to reduce the computation burden without sacrificing too much convergence speed.

4. CONCLUSION

In this paper, we propose a STILC-PID hybrid control method for registration control in an R2R printing system. This method addresses a fundamental challenge in R2R registration control that the control target (registration error) can not be monitored in real-time. When a repetitive disturbance exists, we design a TILC updating law with a spatially dependent basis function to enable the registration to converge to zero iteratively, while the traditional feedback control methods can only make the registration error converge to a non-zero level. To verify the effectiveness of the proposed method, we apply it to a registration control problem in R2R printing systems. The dynamics of the registration error and the R2R system are modeled by the perturbation method. We introduce a spatial-information-dependent disturbance caused by axis mismatch between the motor shaft

TABLE 2: CONTROLLER SETTINGS

Setting	Notation	Value
PID Gain (P)	K_i^P, K_{i+1}^P K_i^I, K_i^I	[-0.1916 0]
PID Gain (I)	$K_i^I, K_{i+1}^{I^{-1}}$	[-0.1150 0]
PID Gain (D)	K_i^D, K_{i+1}^D	[-0.0038 - 0.1916]
ILC Learning Gain	P	5000
Basis Function	G	Shown in Fig. 11 (20-step)

and the roller center, which is very common in rotary machine systems. In Simulink, we conduct the simulation experiment to verify the effectiveness of the proposed STILC-PID hybrid control method. The simulation results show the proposed control method can make the registration error converge to zero iteratively, while the traditional decentralized PID method can only make the registration error converge to a non-zero value. We also compare the performances when we use different basis functions in STILC. The simulation results show that discretized cosine basis functions can help the proposed STILC-PID hybrid control method eliminate the registration error iteratively. A basis function with more discretization steps provides a faster convergence speed. For future work, we will improve the method to control the R2R registration with more practical disturbances, such as roundness errors of rollers and axis mismatches with different initial phase angles. We will also do a strict convergence analysis to guarantee the effectiveness of the proposed STILC-PID control method.

ACKNOWLEDGMENTS

This material is based upon work supported by the National Science Foundation under Grant CMMI-1943801 and CMMI-1907250.

REFERENCES

- [1] Kim, Cheol, Jeon, Sung Woong and Kim, Chung Hwan. "Measurement of position accuracy of engraving in plate roller and its effect on register accuracy in roll-to-roll multi-layer printing." *Measurement Science and Technology* Vol. 28 No. 12 (2017): p. 125002.
- [2] Lee, Jongsu, Seong, Jinwoo, Park, Janghoon, Park, Sungsik, Lee, Dongjin and Shin, Kee-Hyun. "Register control algorithm for high resolution multilayer printing in the roll-toroll process." *Mechanical Systems and Signal Processing* Vol. 60 (2015): pp. 706–714.
- [3] Lee, Jongsu, Park, Soosung, Shin, Kee-Hyun and Jung, Hoeryong. "Smearing defects: a root cause of register measurement error in roll-to-roll additive manufacturing system." *The International Journal of Advanced Manufacturing Technology* Vol. 98 No. 9 (2018): pp. 3155–3165.
- [4] Chen, Zhihua, Zhang, Tao, Zheng, Ying, Wong, David Shan-Hill and Deng, Zhonghua. "Fully Decoupled Control of the Machine Directional Register in Roll-to-Roll Printing System." *IEEE Transactions on Industrial Elec*tronics Vol. 68 No. 10 (2021): pp. 10007–10018. DOI 10.1109/TIE.2020.3029476.

- [5] Chen, Zhihua, Zheng, Ying, Zhang, Tao, Wong, David Shan-Hill and Deng, Zhonghua. "Modeling and register control of the speed-up phase in roll-to-roll printing systems." *IEEE Transactions on Automation Science and En*gineering Vol. 16 No. 3 (2018): pp. 1438–1449.
- [6] Kang, Hyunkyoo, Lee, Changwoo and Shin, Keehyun. "Modeling and compensation of the machine directional register in roll-to-roll printing." *Control Engineering Practice* Vol. 21 No. 5 (2013): pp. 645–654.
- [7] Pagilla, Prabhakar R, Siraskar, Nilesh B and Dwivedula, Ramamurthy V. "Decentralized control of web processing lines." *IEEE Transactions on control systems technology* Vol. 15 No. 1 (2006): pp. 106–117.
- [8] Zhou, Minjing, Chen, Zhihua, Zheng, Ying and Zou, Lamei. "Model based PD control during the speed-up phase in roll-to-roll web register systems." *Proceedings of the 33rd Chinese Control Conference*: pp. 5139–5143. 2014. DOI 10.1109/ChiCC.2014.6895815.
- [9] Bristow, Douglas A, Tharayil, Marina and Alleyne, Andrew G. "A survey of iterative learning control." *IEEE control systems magazine* Vol. 26 No. 3 (2006): pp. 96–114.
- [10] Sutanto, Erick and Alleyne, Andrew G. "Norm Optimal Iterative Learning Control for a Roll to Roll nano/micromanufacturing system." 2013 American Control Conference: pp. 5935–5941. 2013. IEEE.
- [11] Sutanto, Erick and Alleyne, Andrew G. "Vision based iterative learning control for a roll to roll micro/nano-manufacturing system." *IFAC Proceedings Volumes* Vol. 47 No. 3 (2014): pp. 7202–7207.
- [12] Han, Jian, Shen, Dong and Chien, Chiang-Ju. "Terminal iterative learning control for discrete-time nonlinear system based on neural networks." 2015 34th Chinese Control Conference (CCC): pp. 3190–3195. 2015. DOI 10.1109/ChiCC.2015.7260132.

- [13] Bu, Xuhui, Liang, Jiaqi, Hou, Zhongsheng and Chi, Ronghu. "Data-Driven Terminal Iterative Learning Consensus for Nonlinear Multiagent Systems With Output Saturation." *IEEE Transactions on Neural Networks and Learn*ing Systems Vol. 32 No. 5 (2021): pp. 1963–1973. DOI 10.1109/TNNLS.2020.2995600.
- [14] Chi, Ronghu, Wang, Danwei, Hou, Zhongsheng and Jin, Shangtai. "Data-driven optimal terminal iterative learning control." *Journal of Process Control* Vol. 22 No. 10 (2012): pp. 2026–2037.
- [15] Han, Jian, Shen, Dong and Chien, Chiang-Ju. "Terminal iterative learning control for discrete-time nonlinear systems based on neural networks." *Journal of the Franklin Institute* Vol. 355 No. 8 (2018): pp. 3641–3658.
- [16] Xu, Jian-Xin, Chen, Yangquan, Lee, Tong Heng and Yamamoto, Shigehiko. "Terminal iterative learning control with an application to RTPCVD thickness control." *Automatica* Vol. 35 No. 9 (1999): pp. 1535–1542.
- [17] Xu, Jian-Xin and Huang, Deqing. "Spatial periodic adaptive control for rotary machine systems." *IEEE Transactions on Automatic Control* Vol. 53 No. 10 (2008): pp. 2402–2408.
- [18] Afkhami, Zahra, Pannier, Christopher, Aarnoudse, Leontine, Hoelzle, David and Barton, Kira. "Spatial Iterative Learning Control for Multi-material Three-Dimensional Structures." *ASME letters in dynamic systems and control* Vol. 1 No. 1 (2021).
- [19] Liu, Yan and Ruan, Xiaoe. "Spatial Iterative Learning Control for Pitch of Wind Turbine." 2018 IEEE 7th Data Driven Control and Learning Systems Conference (DDCLS): pp. 841–846. 2018. IEEE.
- [20] Yang, Lin, Li, Yanan, Huang, Deqing, Xia, Jingkang and Zhou, Xiaodong. "Spatial Iterative Learning Control for Robotic Path Learning." *IEEE Transactions on Cybernetics* (2022).